11th CIRP Conference on Photonic Technologies [LANE 2020] on September 7-10, 2020

Geometrical model and strategy in single and multilayer structures deposited by powder-fed Directed Energy Deposition

Pedro Ramiro[a],*, Mikel Ortiz[a], Amaia Alberdi[a], Aitzol Lamikiz[b]

[a]TECNALIA, Basque Research and Technology Alliance (BRTA), Paseo Mikeletegi 7, 20009 Donostia-San Sebastián, Spain
[b]Department of Mechanical engineering, Faculty of Engineering of Bilbao, University of Basque Country, Alameda de Urquijo s/n 48013 Bilbao, Spain

* Corresponding author. E-mail address: pedro.ramiro@tecnalia.com

Abstract

This work presents a geometrical model of coatings fabricated by powder-fed Directed Energy Deposition (DED) and defines guidelines and manufacturing strategies for multilayered structures based on the geometrical model results. This model obtains as output both the overlapped clad geometry and the dilution area of the coating at different input parameters and defines the strategy of multi-layer structures.
The results of this work validate the model that comes in handy: a) To understand the influence of each parameter and the single clad geometry when fabricating coatings and structures; b) To select the parameters depending on the requirements of the coating like effective thickness and dilution; c) To detect lack of fusion with the substrate due to an excessive overlap percentage; d) To select the deposition strategy and the tool path for additive manufacturing; e) To select the subsequent machining strategy based on the predicted geometry of the model.

Keywords: Directed Energy Deposition; Powder-fed; Coatings; Multilayer Structure; Geometrical model; Deposition Strategy; Ni-based; Alloy 718.

1. Introduction

The powder-fed Directed Energy Deposition (DED) technology is an Additive Manufacturing process that employs a laser beam to create a melt pool in a metallic substrate where the material is injected in powder form. The added material is fused and solidified by creating a high-quality metallurgical union between the substrate and the added material. The desired part is created layer by layer, thus allowing to manufacture near-net-shape parts with complex geometries that must be finished by a machining process.

Currently, there are different powder injection techniques depending on the application and the kinematic configuration of the DED system: the off-axis powder injection when the deposition strategy is unidirectional [1], the continuous coaxial powder injection for vertical configurations [2], the discrete coaxial powder injection when it is necessary to tilt the nozzle in a multidirectional deposition strategy [3] and the inside beam powder injection with an annular laser beam when it is necessary to achieve a wider tilt range comparing to the commercially available nozzles [4].

One of the most relevant challenges of the DED is the geometric uncertainty of the additive process that must deal with the tool in the subsequent machining operation [5]. Although recently, it has been made great progress in the numerical simulation [6-8], a complete model considering all stages and process parameters is still a complex procedure and far from the real status [9] with a high computational cost and time consuming of the simulation [10].

As an alternative, many authors developed empirical geometrical models [11-14] that cannot predict characteristics as the grain size, hardness, and porosity but that are useful for answer pure geometrical requirements as height, width, waviness or thickness of the deposited material trying to reduce significantly the time rely on expensive and time-consuming techniques, such as multiple experimental runs [15].

On the basis of the single clad characteristics (height, width, area and penetration) and based on both the model developed by Ocelík et al. [16] and an own-developed model of the dilution zone, this work validates a geometrical model of coatings fabricated by powder-fed Directed Energy Deposition (DED) and defines guidelines and manufacturing strategies for multilayered structures based on the experimental results.

Nomenclature

A	Area
d_o	Overlap percentage
h	Height
i	Overlapped clad number
O_i	Origin of the overlapped clad i
O_{i+1}	Origin of the overlapped clad i+1
p	Penetration
w	Width
Y_i	Height in the point P of the clad i

2. Materials and methods

2.1. Materials

The material used in the experimental tests as filler and substrate material was the Nickel-based Alloy 718. The filler material consisted of powder with a granulometry between 45 and 150 μm, from Flame Spray Technologies (FST), and the substrate material was in an annealed state. Table 1 presents the chemical composition of the powder and the substrate materials. This Nickel-based alloy presents excellent properties at high-temperature applications (useful up to 980°C), oxidation, and corrosion-resistant properties, and it is widely used in the aeronautical sector.

Table 1. Chemical composition (Wt. %) of Alloy 718 powder and substrate.

	Ni	Cr	Fe	Nb+Ta	Mo	Ti	Al
Powder	52.8	18.5	18	4.8	3.5	0.75	0.3
Substrate	53.5	18.7	17.7	5	2.9	0.94	0.58

2.2. Machine

All tests were performed in an IBARMIA ZVH45/1600 Add+Process hybrid machine (Fig. 1). This multiprocess machine combines the DED technology with 5-axis milling and turning (horizontal and vertical) capability. This machine is equipped with a Precitec YC52 cladding head with a collimating and focusing optics of 125 mm and 250 mm respectively, a Sulzer Metco TWIN-10-C Powder Feeder, and an Yb-Fiber Rofin FL030 Laser generator of 3 kW with a continuous wavelength of 1.07 μm. For nozzle, a 4-stream coaxial discrete nozzle from Precitec was used.
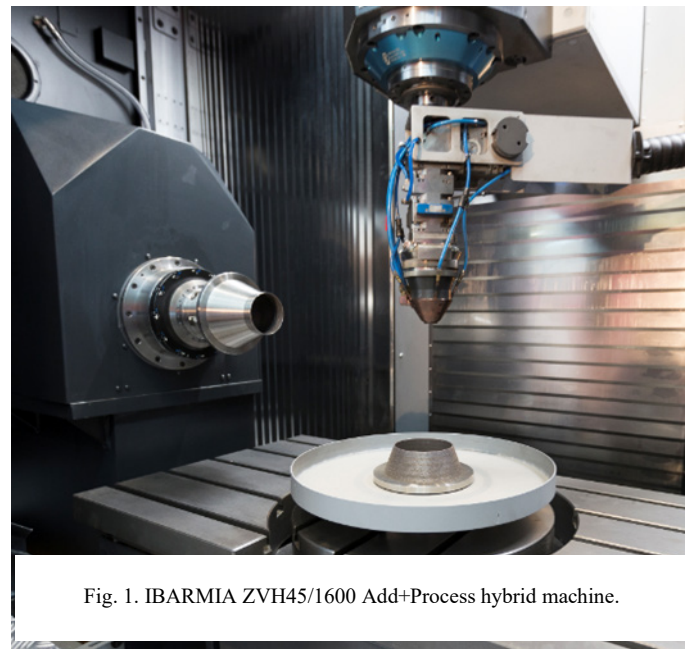
2.3. Geometrical model of single layer coatings

This work proposes a model for the overlapped clad based on the model developed by Ocelík et al. [16], supposing that each new clad of the coating has a second-degree parabolic shape. This model achieved a high level of accuracy by taking into account purely geometrical parameters such as the characteristics of the single clad (Fig. 2) and the overlap percentage (d_o) of the coating.

The model supposes that each new clad is deposited with the same characteristics than the single clad (Fig.3.a) forming a new clad i+1 with the overlapped area of the previous clad i (Fig. 3.b). This clad i+1 is calculated by assuming the height Y_i in the overlapped point P is the same as in the previous (clad i) and it has a second-degree parabola shape with a higher width (w_{i+1}). The area from the origin O_{i+1} to P is the sum of the single clad area and the overlapped area of the previous clad i. The distance from the from the origin O_{i+1} to P is the same than the single clad width (w). In the first iteration, the clad i is the single clad.
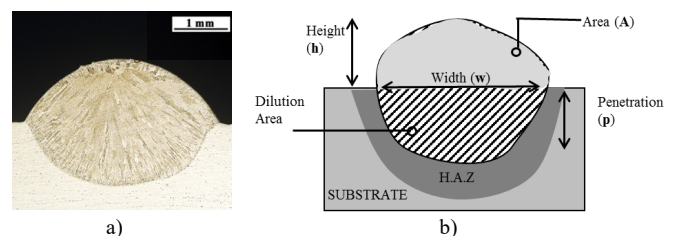

Fig. 2. Single clad: a) Macro photograph of a cross-section of a single clad; b) Single clad characteristics.
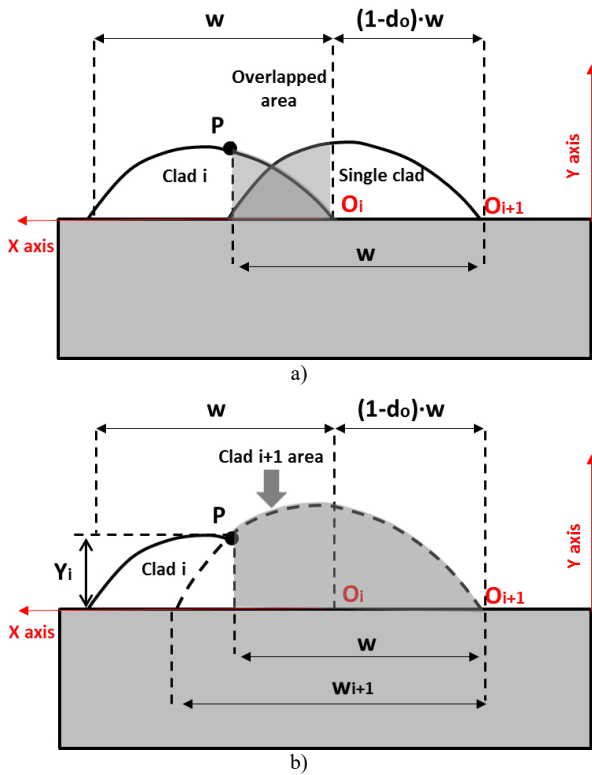
Fig. 3. Geometrical model of the deposited material. a) Clad deposited overlapping the previous clad; b) Clad i+1 of the model.

Furthermore, to complete the model, it is proposed a simple model of the dilution zone of the overlapped clad based on experimental results of previous works [17-19].

This model simplifies the real dilution of the clad (Fig. 4.a) to a second-degree parabola in the substrate (Fig. 4.b) and supposes that the sum of the height and penetration remain constant in all the clads that belong to the coating (eq.1). This assumption is a simplified form of energy balance between the deposited material and the melted substrate and it was obtained by analysing all the fabricated coatings in previous works with different nozzles, metallic powders and substrates.

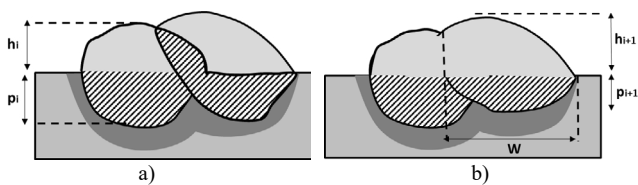$$h_i + p_i = h_{i+1} + p_{i+1} \qquad (1)$$

Fig. 4. Dilution of the adjacent clad i+1. a) Real; b) Model.

The model serves to calculate and simulate the geometry of the coatings and the dilution area, including the prediction of lack of fusion with the substrate due to a high overlap percentage, by knowing the height, area, width and penetration of the single clad. In addition, the characteristics of the single clad can be estimated using empirical models obtained in previous works [17-18].

2.4. Strategy for multilayer coatings

When fabricating a multilayer structure with more than two clads per layer, the coating thickness increases from the first clad until it reaches to constant thickness. In addition, the last clad presents a sharp curve from the top to the substrate. Both situations generate a lack of material on the edges (Fig. 5.a), generating a distortion on the edges that increases at a higher number of layers.

This work proposes to deposit one extra clad on the edge of the layer to compensate this phenomenon of lack of material. The model can be used to predict the area needed on the edges of the layer to obtain a constant growth without distortions. The growth per layer it is the constant thickness obtained supposing a coating formed by rectangular blocks at the same area than the area within the overlapped parts of the model (Fig. 5.b). The extra clad area is the needed area to obtain a constant thickness in each edge.
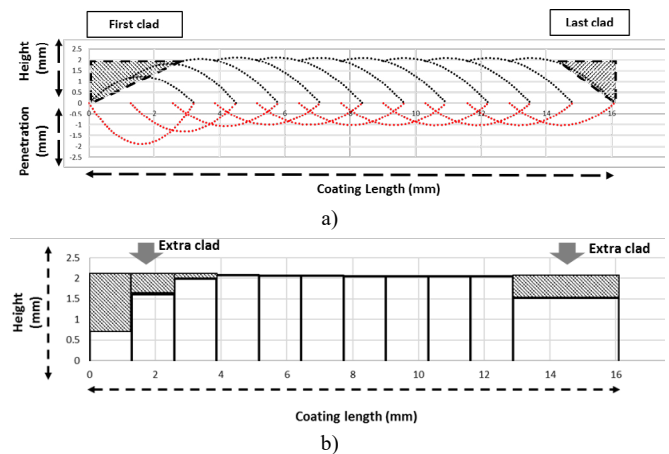

Fig. 5. Lack of material predicted by the model in the edges of the layer. a) Second degree parabola shape; b) Supposing rectangular blocks.

The extra clad parameters must be calculated depending on the area needed for a straight growth. The simplest way to obtain them is to adapt the feed rate maintaining the same laser power and powder mass flow rate. This occurs because the area of the single clad presents a linear trend with the inverse of the feed rate [17-18]. The area of the extra clad needed per layer is significantly lower than the area of the clad used for coating. Thus, the extra clad must be deposited at higher feed rates. As the powder efficiency is lower at higher feed rate, it was determined to deposit one extra clad every two layers with twice the calculated area to obtain an extra clad with similar feed rate (thus, similar efficiency) to the coating clads. The accuracy of the model depends on the accuracy of the single clads characteristics.

2.5. Experimental validation

To validate the model when employing Alloy 718 with the 4-stream nozzle three coatings of Alloy 718 were deposited for

validating the model. Each coating was done overlapping 8 clads employing different single clads characteristics (Table 2). The cross-sections of the coatings were compared with the model, and the error was calculated.

Table 2. Single clad characteristics of each coating.

Single clad Characteristics	Coating 1	Coating 2	Coating 3
h (mm)	1.22	0.63	0.88
w (mm)	3.22	2.72	2.90
A (mm^2)	2.63	1.15	1.68
p (mm)	1.88	1.25	1.61
d_o (%)	40	50	60

The distance from the 4-stream coaxial discrete nozzle to the substrate was 14.5 mm. As a carrier and protective gas, 4.5 and 18 l·min^{-1} of argon flow were used respectively. Finally, a spot size of 2.6 mm was employed.

After the validation of the geometrical model, two walls were fabricated at the same conditions (Table 3) with and without extra clads to compare the results and thus, for validating the proposed strategy for multilayer coatings. The extra clads were added in the edges of the wall every two layers at the same parameters than the rest of the clads excepting a feed rate of 600 mm·min^{-1} to obtain the calculated area by the model for correct growth. The wall was fabricated with 12 layers, the growth per layer was 1.3 and the number of clads per layer was 6.

Table 3. Straight wall parameters.

Laser Power (W)	Feed rate (mm·min^{-1})	Powder mass flow (g·min^{-1})	d_o (%)
2500	500	18	40

3. Results and discussion

3.1. Validation of the geometrical model

The obtained results were close to the real cross-section in all coatings (Fig. 6). The maximum deviation of the real coating thickness and the model was 0.14 mm. In the case of the penetration, although most of the overlapped clads are close to the model, the deviation reaches 0.3 mm in one of them, due to the process variability. The maximum deviation of the real value of the coating thickness and penetration are calculated, and it is shown in Table 4.
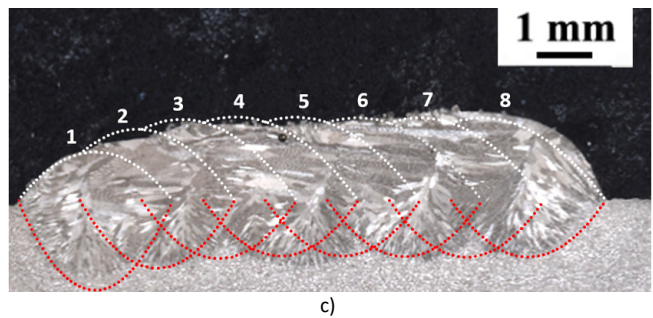

a)

b)

c)

Fig. 6. Real Coatings macrographs compared with the model: a) Coating 1; b) Coating 2; c) Coating 3.

Table 4. Coatings thickness and penetration: maximum and minimum deviation of the real section regarding the model.

Coating Characteristic	Error (mm)	Coating 1	Coating 2	Coating 3
Thickness	Maximum deviation	0.14	0.1	0.13
Penetration		0.3	0.25	0.19

3.2. Validation of the strategy for multilayer coating

In the case of the multilayer structures (Fig. 7), the wall deposited with the extra clad strategy presents a rectangular shape without distortions in the edge and a total wall height close to expected with low variability. The obtained structure allows to deposit accurately more layers.

On the contrary, the wall deposited without the extra clad presents a high distortion with a bullet shape. The distortion increases sharply at a higher number of layers.

In addition to the loose of the geometrical accuracy, this distortion has one additional effect over the material deposition: the decrease on the powder efficiency. In fact, the powder efficiency of the first structure was 52.4%, while it increased to a 60.1% in the structure with extra clads.
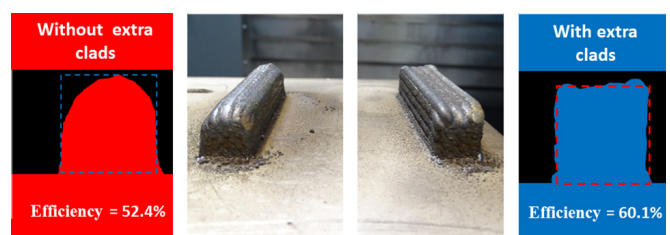

Fig. 7. Straight wall results. In red, cross-section without extra clad strategy; In blue, cross-section with extra clad strategy.

4. Conclusions and future work

The model allows to select the single clad geometry and the overlapped percentage for a determinate thickness or dilution of the coating based on pure geometrical characteristics of the single clad. At higher accuracy of the single clad characteristics, higher accuracy of the model can be obtained.

The model could also determine the possible maximum thickness without a lack of fusion due to an excess of overlap.

The accuracy of the model allows to select the tool path of the machining process and predicts the material that is necessary to remove until it reaches to a constant thickness,
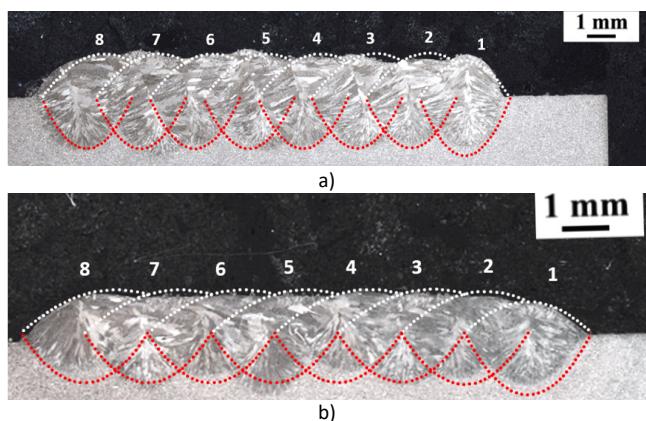
In addition, thanks to the extra clad strategy, it has been demonstrated that it is possible to obtain constant growth when fabricating a multilayer structure, which increases also the powder efficiency of the process.

In future works, it would be advisable to address the following aspects:

- To develop geometric models for coatings and walls using the equations for the single clad characteristics and the evolution of the characteristics linked to head tilting and non-perpendicularity.
- To use the models that are developed to manufacture walls of variable thickness.
- To include the models developed in Computer-Aided Manufacturing software, in order to calculate the DED process toolpath, the Computer Assisted Design expected from the DED process and the subsequent machining toolpath.

Acknowledgments

References

[1] Ur Rahman, N.; Capuano, L.; Van der Meer, A. et al. (2018). Development and characterization of multilayer laser cladded high speed steels. Additive Manufacturing, 24, 76-85. DOI: http://doi.org/10.1016/j.addma.2018.09.009

[2] Zhong, C.; Pirch, N.; Gasser, A. et al. (2017). The Influence of the Powder Stream on High-Deposition-Rate Laser Metal Deposition with Inconel 718. Metals, 7 (10), 443. DOI: http://doi.org/10.3390/met7100443

[3] Ramiro-Castro, P.; Ortiz, M.; Alberdi, A. et al. (2020). Effects of Gravity and Non-Perpendicularity during Powder-Fed Directed Energy Deposition of Ni-Based Alloy 718 through Two Types of Coaxial Nozzle. Metals, 10, 560. DOI: https://doi.org/10.3390/met10050560

[4] Zhu, G.; Shi, S.; Fu, G. et al. (2017). The influence of the substrate-inclined angle on the section size of laser cladding layers based on robot with the inside-beam powder feeding. Int J Adv Manuf Technol, 88 (5-8), 2163-2168. DOI: https://doi.org/10.1007/s00170-016-8950-4

[5] Cortina, M.; Arrizubieta, J.I.; Ruiz, J.E. et al. (2018). Latest Developments in Industrial Hybrid Machine Tools that Combine Additive and Subtractive Operations. Materials, 11, 2583. DOI: https://doi.org/10.3390/ma11122583

[6] Arrizubieta, J.I.; Lamikiz, A.; Cortina, M. et al. (2018). Hardness, grainsize and porosity formation prediction on the Laser Metal Deposition of AISI 304 stainless steel. Int. J. Mach. Tool Manufact., 135, 53-64. DOI: https://doi.org/10.1016/j.ijmachtools.2018.08.004.

[7] Wei, H.L.; Knapp, G.L.; Mukherjee, T. et al. (2019). Three-dimensional grain growth during multi-layer printing of a nickel-based alloy Inconel 718. Additive Manufacturing, 25, 448-459. DOI: https://doi.org/10.1016/j.addma.2018.11.028.

[8] Lu, X.; Lin, X.; Chiumenti, M. et al. (2019). Residual stress and distortion of rectangular and S-shaped Ti-6Al-4V parts by Directed Energy Deposition: Modelling and experimental calibration. Additive Manufacturing, 26, 166-179. DOI: https://doi.org/10.1016/j.addma.2019.02.001.

[9] Tamanna, N.; Crouch, R. and Naher, S. (2019). Progress in numerical simulation of the laser cladding process. Optics and Lasers in Engineering, 122, 151-163. DOI: https://doi.org/10.1016/j.optlaseng.2019.05.026.

[10] Salonitis, K.; D'Alvise, L.; Schoinochoritis, B. et al. (2016). Additive manufacturing and post-processing simulation: laser cladding followed by high speed machining. Int. J. Adv. Manuf. Technol., 85 (9-12), 2401. DOI: https://doi.org/10.1007/s00170-015-7989-y

[11] Bax, B.; Rajput, R.; Kellet, R. et al. (2018). Systematic evaluation of process parameter maps for laser cladding and directed energy deposition. Additive Manufacturing, 21, 487-494. DOI: https://doi.org/10.1016/j.addma.2018.04.002.

[12] El Cheikh, H., Courant, B., Branchu, S. et al. (2012). Analysis and prediction of single laser tracks geometrical characteristics in coaxial laser cladding process. Optics and Lasers in Engineering, 50 (3), 413-422. DOI: https://doi.org/10.1016/j.optlaseng.2011.10.014.

[13] Chen, T.; Wu, W.; Li, W. et al. (2019). Laser cladding of nanoparticle TiC ceramic powder: Effects of process parameters on the quality characteristics of the coatings and its prediction model. Optics & Laser Technology, 116, 345-355. DOI: https://doi.org/10.1016/j.optlastec.2019.03.048.

[14] Zhang, K.; Wang, S.; Liu, W. et al. (2014). Characterization of stainless steel parts by Laser Metal Deposition Shaping. Materials & Design, 55, 104-119. DOI: https://doi.org/10.1016/j.matdes.2013.09.006.

[15] Dass, A.; Moridi, A. (2019). State of the Art in Directed Energy Deposition: From Additive Manufacturing to Materials Design. Coatings, 9, 418. DOI: https://doi.org/10.3390/coatings9070418

[16] Ocelík, V.; Nenadl, O.; Palavra, A. et al. (2014). On the geometry of coating layers formed by overlap. Surface and Coatings Technology, 242, 54-61. DOI: https://doi.org/10.1016/j.surfcoat.2014.01.018.

[17] Ramiro, P., Ortiz, M., Alberdi, A. et al. (2018). Characteristics of Fe-based powder coatings fabricated by laser metal deposition with annular and four stream nozzles. Procedia CIRP, 74, 201-205. DOI: https://doi.org/10.1016/j.procir.2018.08.094

[18] Ramiro, P., Alberdi, A., Ortiz, M. et al. (2018). Characteristics of Fe-, Ni- and Co-based powder coatings fabricated by laser metal deposition without preheating the base material. Procedia CIRP, 68, 381-386. DOI: https://doi.org/10.1016/j.procir.2017.12.099

[19] Ramiro, P., Ortiz, M., Alberdi, A. et al (2018). Optimization of the efficiency of the laser metal deposition process applied to high hardness coatings by the analysis of different types of coaxial nozzles. DYNA, 93(6). 613-619. DOI: http://dx.doi.org/10.6036/8836